A Low-Power and In Situ Annealing Mitigation Technique for Fast Neutrons Irradiation of Integrated Temperature Sensing Diodes

Laurent A. Francis, *Member*, *IEEE*, Nicolas André, *Member*, *IEEE*, Pierre Gérard, S. Zeeshan Ali, *Member*, *IEEE*, Florin Udrea, *Member*, *IEEE*, and Denis Flandre, *Senior Member, IEEE*

***Abstract*– High doses of fast neutrons is detrimental to the performance of most common solid-state devices such as diodes and transistors. The ionizing effect is observed in particular for diodes used as simple integrated temperature sensors, or thermodiodes, when their junction voltage is measured at constant current bias. In this work, we present a low-power and *in situ* mitigation technique based on Silicon-on-Insulator (SOI) microhotplates to recover thermodiodes. The basic operating principle consists in annealing the temperature-sensitive diodes integrated on the membrane during or after their irradiation in order to restore similar sensing characteristics over time. We measured thermodiodes integrated to microhotplates during their irradiation by fast neutrons (23 MeV peak) with total doses about 2.97±0.08 kGy. The membrane annealing is taking place at 450 °C using 40 mW of electrical power. Thanks to the annealing, the diode keeps a total measurement error below 0.5 °C. In this harsh radiation environment and beside the good tolerance of the thermodiodes and the membrane materials to the total ionizing dose, the thermodiode located on the heating membrane keeps a constant sensitivity. The demonstrated resistance of micro-hotplates and the integrated thermodiodes to fast neutron radiations can extend their use in nuclear plants and for radiation detectors.**

I. Introduction

High doses of fast neutrons, with their resulting secondary ionization and structural damages, is detrimental to the performance of most common solid-state devices such as diodes and transistors. In particular, diodes can be used as simple integrated temperature sensors when their junction voltage is measured at constant current bias. To prevent the devices degradation, different radiation hardening techniques are already available at hand and rely on a restricted selection of materials, on specific fabrication processes, on improved designs, on predictive models, or on dedicated packaging [1-8]. All of them present their own advantages and drawbacks; they often come at higher specific costs and with particular reliability issues.

In this work, we present a low-power and *in situ* mitigation technique based on microhotplates. These are microelectromechanical (MEMS) structures of interest for low-power gas sensing, lab-on-chips and space applications, such as microthrusters [9]. They usually consist in a Joule heater formed by a metal or a doped polysilicon meander resistor suspended on a dielectric thin-film membrane, such as silicon oxide or silicon nitride or a combination of both in order to reduce the strain and the buckling of the framed membrane [10]. This material combination allows to heat up the resistor to elevated temperatures, such as 400 °C and above, without damaging the structure and with a moderate electrical power requirement, such as a few tens of mW, depending upon the configuration and the design of the membrane and the resistor. Thermopiles or thermodiodes can be added as temperature sensors and for feedback control.

Microhotplates are fabricated using standard complementary metal-oxide-semiconductor (CMOS) technology with a tailored silicon bulk etching of the backside of the membrane. This etching is done either by wet or by dry etching techniques, e.g. KOH or TMAH solutions wet etching, or deep reactive ion etching (DRIE, or Bosch process). This fabrication approach allows the monolithic integration of the heated membrane with thermopiles or thermodiodes. For this latter case, Silicon-On-Insulator (SOI) substrates are preferred over bulk silicon substrates as the buried oxide layer acts as a direct etch-stop layer during the membrane etching and the active silicon layer can embed the thermodiodes in the membrane area. The bulk area can be devoted to other analog integrated circuits as driving interface and feedback control for the heater and the sensing thermodiodes. Beside that, SOI technology integrated circuits have demonstrated superior performances and increased robustness over standard bulk silicon at elevated environmental temperatures in a range from 200 to 300 °C, making this technology particularly attractive for applications in harsh environments [11-12].

To be operated as gas sensor [10,13], the membrane must be modified to include electrodes in contact with metal-oxide materials on the top surface that provide resistive variations

Manuscript received April 6, 2015. This work was supported in part by EU FP7 SOI-HITS (Smart Silicon- on-Insulator Sensing Systems Operating at High Temperature) – see www.soi-hits.eu.

L.A. Francis, N. André, P. Gérard, and D. Flandre are with the Institute of Information and Communication Technologies, Electronics, and Applied Mathematics, Université catholique de Louvain, B-1348 Louvain-la-Neuve, Belgium (e-mail: {laurent.francis},{nicolas.andre},{pierre.gerard}, {denis.flandre}@uclouvain.be). L.A. Francis is corresponding author.

F. Udrea is with Department of Engineering, Electrical Engineering Division, University of Cambridge, 9 JJ Thomson Avenue, CB3 0FA, Cambridge, United Kingdom (e-mail: florin.udrea@ucam.uk).

S.Z. Ali and F. Udrea are with Cambridge CMOS Sensors, Ltd., St Andrew's House, CB2 3BZ, Cambridge, United Kingdom (e-mail: zeeshan.ali@ccmoss.com)

depending upon the exposed gases and their concentration. The metal-oxide layer provides the gas selectivity and requires to be activated at elevated temperature (400 to 600 °C) in order to conduct electricity significantly. The gain of a membrane with respect to a more standard implementation of electrodes on a bulk ceramic support resides in the low thermal inertia and the low thermal loss of the membrane that allows to reach high temperatures with a good linearity and a few mW-range electrical power [14]. This opens the application of microhotplates to low power gas sensors.

The implementation of microhotplates using SOI technology makes them suited for co-integration with analog integrated circuits and operation at elevated environmental temperatures in a range from 200 to 300 °C, while the heater combined to the low thermal inertia of the membrane allows rapid thermal cycling in the ms-range up to 700 °C with mW range electrical power. Thus, the basic operating principle proposed here consists in the annealing the temperature-sensitive diodes integrated on the membrane during or after their irradiation in order to restore similar sensing characteristics over time.

The resistance of microhotplates to ionizing radiations is a motivation to extend their use in nuclear plants and research fields, biomedical sterilization [15-16] and space applications. The requirements are different for each considered environment, with a large variety of constraints extending much over the simple resistance to the radiation level, whereas temperatures, vibrations, shocks, pressure, etc., may also co-exist. Fast neutron radiations, as any other ionizing radiations, are harmful for standard integrated circuits devices due to the ionizing process that generates trapped charges in the gate oxide [17]. This effect deteriorates their operation and result in malfunctions for most CMOS devices. As MEMS devices have already attracted attention for their good behavior in harsh environments [18-19], SOI-based microhotplate under fast neutron irradiation is in the direct scope of this investigation as a step forward the fabrication of a fully-integrated low-power gas sensor for such harsh environment applications.

II. Experimental Methodology

The experimental methodology consisted in the preparation of three identical devices, labeled here A, B and C. The devices are designed to contain two p+/p/n+ diodes in the active layer of a Silicon-On-Insulator (SOI) substrate and a serpentine tungsten resistor as thermal heater. The devices have been fabricated using the 1.0 µm non-fully depleted Silicon-On-Insulator (XI 10) foundry service provided by X-FAB (Erfurt, Germany). Design considerations and temperature performance of these devices can be found in Ref. [20], while a schematic cross-section of the device build-up is shown in Fig. 1 and the layer thicknesses are provided in Table 1. All the diodes are identical with a 5 μm^2 junction area, a width of 20 µm and a length of 10 µm. A circular membrane with a diameter of 600 µm has been post-processed using DRIE process to support one of the two diodes on each chip. The tungsten heater is surrounding the diode supported on the membrane to allow rapid thermal cycles from room temperature up to 600 °C. The final fabricated devices, photographed in Fig. 2, are then two diodes as temperature sensors, one of them located on a microhotplate and the other one located on the bulk substrate.

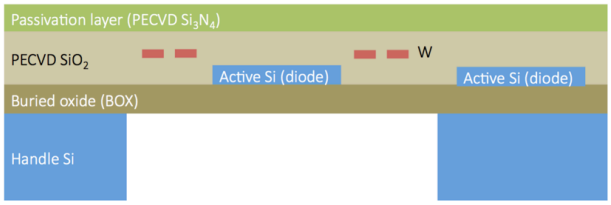

Fig. 1. Schematic (not to scale) cross-section of the microhotplate indicating the stack of layers (PECVD stands for plasma-enhanced vapor chemical deposition, the buried oxide is a thermal oxide).

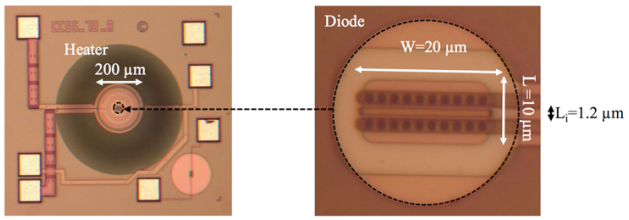

Fig. 2. (To the left) Top view micrograph of the SOI microhotplate showing the dimensions of the heated area, the positions of the membrane and the bulk thermodiodes. (To the right) Magnified view of the thermodiode. The membrane is circular with a diameter of 600 µm.

TABLE 1. MICRO-HOTPLATES MATERIALS THICKNESS.

Material	**Thickness**
PECVD Si_3N_4 (passivation)	500 nm
PECVD SiO_2	3 µm
Tungsten heater	500 nm
SOI Si active layer (diode)	250 nm
Buried oxide (BOX)	1 µm
Handle Si (SOI substrate)	380 µm

The fabricated microhotplates were packaged in closed DIL-16 ceramic packages and embedded in three identical test printed circuit boards (PCBs). The current-tension (I-V) of the diodes was recorded during irradiation testing (HP4156 Semiconductor Parameter Analyzer, Agilent), connected to the PCBs by 1-m long coaxial cables to a distribution box and then to 9-m long twisted coaxial cables. The voltage sweep was varied from -2 V to +1 V by steps of 25 mV with a 1 mA compliance. Each voltage step was measured three times. The three devices were measured subsequently by switching between them after each data acquisition with the help of a switch matrix (E5250A Low Leakage Switch Mainframe, Agilent). For heating the membrane, a coaxial cable was used to power the microheater of the devices from the same Parameter Analyzer from 0 to 2 V, and back, by steps of 250 mV with a 18.2 mA compliance in order to limit the membrane temperature to about 450 °C. The devices B and C were both kept at ambient temperature during the entire irradiation experiment.

The I-V curves were continuously measured and logged with a home-made interface operating under LabWindows™ before, during, and after the irradiation experiment. For comparison

purpose, the heating was performed on device B before irradiation and on device A during irradiation. The noise floor is in the order of 1 pA during the measurements out of the radiation chamber, and of 100 pA while in the radiation chamber because of cross-talks.

Neutron irradiations were performed at room temperature (Cyclotron Research Centre at the Université catholique de Louvain, Louvain-la-Neuve, Belgium), using the high-flux fast neutron beam facility. The neutron line uses a primary 50 MeV deuteron beam on a beryllium target, with the high cross-sectional reaction ^{9}Be(d, n)^{10}B producing the high-flux neutron beam [21]. The neutron production beryllium target is electrically insulated from the rest of the beam line. The deuteron current is monitored on the target, and it can also be used for the evaluation of the neutron fluence.

To keep the gamma and charged particle contamination as low as possible, a three-layer filter composed of 1-cm-thick polyethylene, 1-mm-thick cadmium, and 1-mm-thick lead is used. The filter diminishes the relative amount of charged particles and is also effective in capturing the low-energy neutrons from the beam albeit at the expense of increasing the relative amount of accompanying gamma radiation up to 2.4%. The energy spectrum of the outcoming neutron beam is ranged from 5 to 45 MeV dominated by a peak in the region of 23 MeV. Aside from the deuteron current online monitoring, Bruker® alanine pellet dosimeters are placed in front of each packaged device [22]. The radiation produces stable free radicals that are measurable quantitatively by electron spin resonance technique. The neutron dose response of the alanine probes relative to the response of ^{60}Co in silicon is taken from [46]. The experimental results are obtained from electrical tests on the thermodiodes integrated to the microhotplates during their irradiation by fast neutrons with a total dose about 2.97±0.08 kGy, as measured by the alanine dosimeters. The corresponding neutron fluence is $7 \cdot 10^{13}$ n/cm^2.

III. Results

Fig. 3 shows the evolution of the current in the non-heated membrane diodes (devices B and C) and the bulk diodes (devices A, B and C) for a forward voltage bias arbitrarily set at 700 mV for illustration and as a function of the total ionizing dose (TID). As expected from the literature, the current is increasing due to the ionizing effects of the neutron irradiation bringing trapped charges in the oxide. The cumulative effect is leading to a saturation of the current shifting for the highest total dose. The trend is the same in all observed diodes, whether located on the bulk or on the membrane. The current in the bulk diode of device A, which is thermally cycled during the experiment, has slight fluctuations linked to the direct thermal coupling between the membrane and the bulk.

Fig. 4 shows the same situation for the heated membrane diode of device A. The temperature of the membrane was cycled from room temperature up to about 450 °C continuously during the entire duration of the experiment. While the current is drastically modified due to the temperature, one can observe that an annealing due to the Joule effect is preventing the membrane diode to follow the degradation seen in the other diodes. However, the performance of the diode remains constant over time.

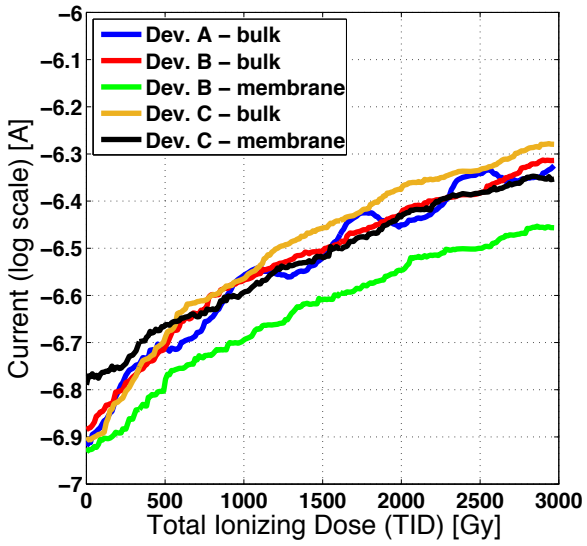

Fig. 3. Current measured for a forward bias voltage of 700 mV in the non-heated thermodiodes as a function of the total ionizing dose.

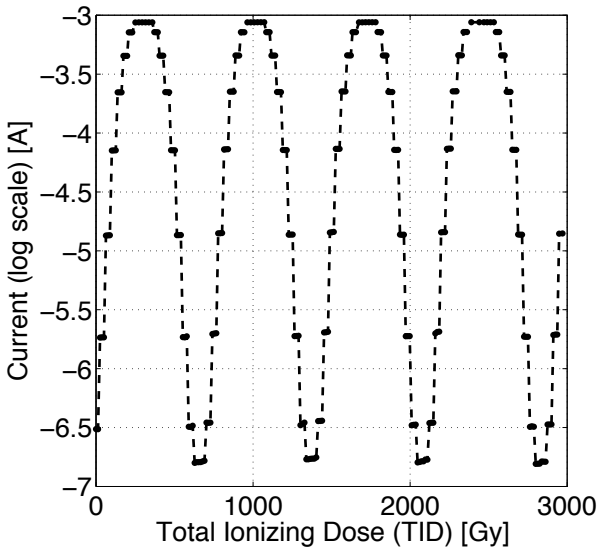

Fig. 4. Current measured for a forward bias voltage of 700 mV in the heated thermodiode on the membrane of the micro-hotplate as a function of the total ionizing dose.

As we have measured the entire I-V curves, data post-treatment allows extracting the actual voltage shifts for a given current. For the bias currents I (in [A]), the measured voltage is approximated by a linear regression as a function of the TID (in [Gy]) under the form:

$$V(I,\mathrm{TID}) = [a \cdot \log(I) + b] \cdot \mathrm{TID} + c \cdot \log(I) + d$$

The computation has been performed and is valid only for currents between 0.1 µA and 100 µA. Table 2 provides the expression of the regression coefficients *a*, *b*, *c*, and *d*.

TABLE 2. LINEAR REGRESSION COEFFICIENTS OF THE VOLTAGE AS A FUNCTION OF THE FORWARD BIAS CURRENT AND THE TOTAL IONIZING DOSE FOR THE DIFFERENT NON-HEATED THERMODIODES.

Dev.	Diode	*a* [10^{-6} V/A/Gy]	*b* [10^{-5} V/Gy]	*c* [10^{-2} V/A]	*d* [V]
A	Bulk	6.07	2.54	6.96	1.17
B	Bulk	6.18	2.61	7.09	1.18
B	Memb.	4.09	1.64	6.58	1.15
C	Bulk	6.18	2.52	7.07	1.17
C	Memb.	3.59	1.34	6.99	1.17

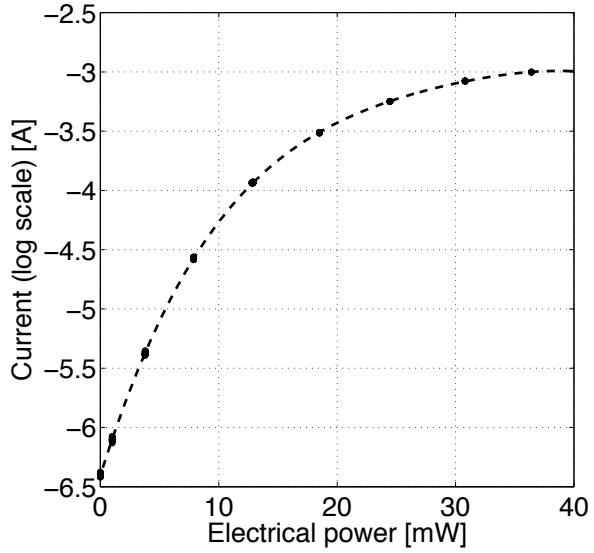

Fig. 5. Measured current for a forward bias voltage of 700 mV in the heated thermodiode on the membrane as a function of the electrical power injected in the microheater. The dashed line is a 4th degree polynomial regression of the data points collected during the entire irradiation experiment.

Fig. 5 shows the relationship between the power injected in the microheater and the current in the membrane diode of device A for all measured points during the irradiation. A 4th degree polynomial regression curve is used to fit the data. The power is related to the actual temperature in the membrane with a value of 40 mW heating the membrane up to about 450 °C. The graph shows the reproducibility of the diode measurement for the same injected power in the heater despite the ongoing irradiation process, we can thus reliably obtain the temperature in the membrane thanks to this diode. A safe assumption is related to the unmodified electrical properties of the heater material, tungsten, due to the neutron irradiation.

Operated as thermodiode, the voltage shift as a function of the temperature is monitored for a constant forward bias current. The nominal bias current is set to 65 µA. For the thermodiode on the membrane of device A, the relationship between the electrical power *P* injected in the heater (in [W]) and the voltage is provided by a linear regression as well:

$$V(I,P) = \beta(I) \cdot P + 7.15 \cdot 10^{-2} \cdot \log(I) + 1.16$$

where

$$\beta(I) = 1.87 \cdot \log(I) - 4.56$$

For this device design, there is a roughly linear relationship between the membrane temperature *T* (in [°C]) and the electrical power *P* (in [W]) dissipated by the microheater in the form $T(P)=T_0+1.05\cdot10^4P$, where T_0 is equal to 25 °C, while the temperature dependence of the thermodiode can be written as $V(T) = V_0 + \alpha(I) \cdot (T-T_0)$, where V_0 is the forward bias voltage at 25 °C and $\alpha(I)$ the temperature coefficient (or temperature sensitivity) of the diode, function of the forward bias current. To be consistent with our present approach, the temperature coefficient is replaced by a power sensitivity slope $\beta(I)$ such that $V(P) = V_0 + \beta(I)P$. Obviously, $\alpha(I) = \beta(I)/1.05\cdot10^4$ for this specific device design of the microheater and the membrane. By replacing the expression for $\beta(I)$, the thermodiode has a temperature coefficient that span from –1.68 mV/°C at 0.1 µA to –1.15 mV/°C at 100 µA. The different thermodiodes have similar temperature coefficients.

Fig. 6 represents the maximal absolute error on the temperature measurement for the thermodiode on the membrane as a function of the bias current in the absence of heating. This shows that in the nominal operation the error is limited to 0.28 °C.

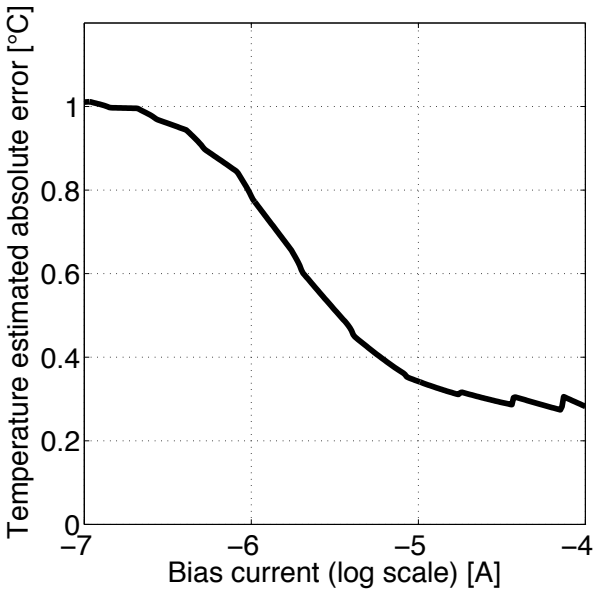

Fig. 6. Estimation of the maximum absolute error on the temperature measurement vs. bias current for the heated membrane thermodiode at null power of the heater.

Figs. 7 and 8 are providing the estimation of the temperature error as a function of the total ionizing dose for the six measured diodes with reference to the irradiation starting point. The error is increasing linearly as the total dose is increasing, although the heated membrane is recovering its initial performance and a low maximum error, below 0.23 °C.

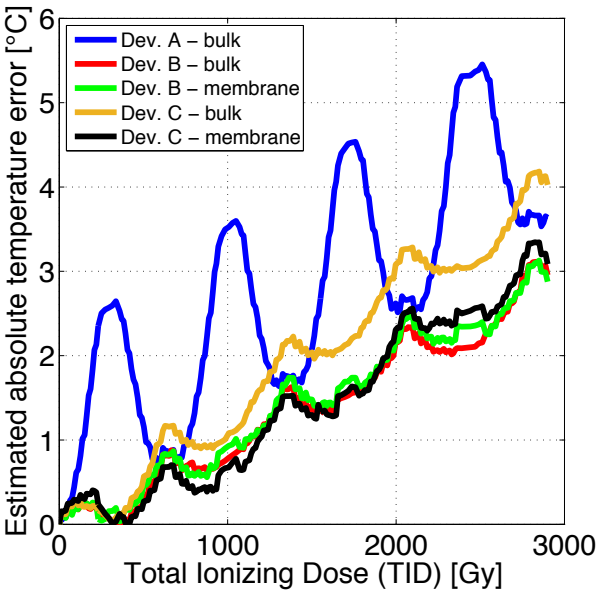

Fig. 7. Estimation of the maximum absolute error on the measurement for the different thermodiodes (except the heated one) for a bias current of 65 µA vs. total ionizing dose.

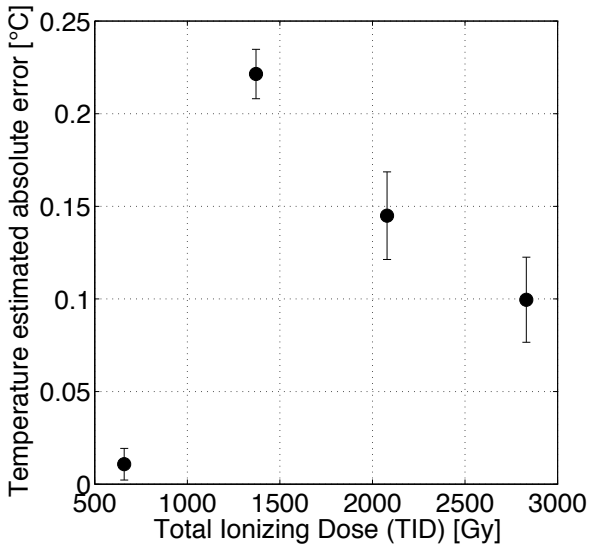

Fig. 8. Estimation of the maximum absolute error on the temperature measurement for a bias current of 65 µA of the thermodiode for the heated membrane at null power of the heater vs. total ionizing dose.

IV. Conclusions

Microhotplates presented here are MEMS devices fabricated with a standard 1.0 µm non-fully depleted Silicon-On-Insulator technology that can embed thermodiodes as temperature sensitive elements for feedback control. These micro-hotplates have demonstrated robustness to fast neutrons irradiation with a total ionizing dose up to 2.97±0.08 kGy (equal to a fluence of $7 \cdot 10^{13}$ n/cm^2). However, the ionizing irradiation induces trapped charges in the oxide that causes I-V shifts of the thermodiodes and result in an absolute measurement error above 3 °C on the temperature estimation, the error will ever increase for even larger doses.

This drawback can be compensated by annealing the thermodiode located on the membrane of the microhotplate from room temperature to about 450 °C. Thanks to a low thermal dissipation, the annealing is performed by the microheater on the membrane with an electrical power of 40 mW sufficient to restore the original diode characteristics and reduce the measurement error. At a nominal value of the forward bias current set to 65 µA, the temperature sensitivity is equal to –1.18 mV/°C, the precision of the measurement at room temperature is less than 0.28 °C and the irradiation effect is limited to an extra 0.23 °C measurement error. The total absolute error is thus lower than 0.51 °C. The annealing step can be performed at any stage, during or after exposure to the fast neutrons.

In this harsh radiation environment and beside the good tolerance of the thermodiodes and the membrane materials to the total ionizing dose, the thermodiode located on the heating membrane is constantly annealed during irradiation and keeps a constant sensitivity. The demonstrated resistance of microhotplates and the integrated thermodiodes to fast neutron radiations can extend their use in nuclear plants and for radiation detectors.

Acknowledgment

The authors are thankful to the technical team of the CYCLONE Irradiation Facility at UCL for the assistance with irradiation set-up, and to Loïc Van Oldenheel tot Oldenzeel and David Spôte at UCL for the test PCBs fabrication.

References

[1] X. Han, L. Wu, Y. Zhao, Y. Li, Q. Zhang, L. Chen, G. Zhang, J. Li, B. Yang, J. Gao, J. Wang, M. Li, G. Liu, F. Zhang, X. Guo, L.C. Stanley, Z. Liu, F. Yu, K. Zhao, "A radiation-hardened SOI-based FPGA," *J. Semicond.*, vol. 32, no. 7, art. no. 075012, 2011.

[2] C. Da Viá, J. Hasi, C. Kenney, V. Linhart, S. Parker, T. Slavicek, S.J. Watts, P. Bem, T. Horazdovsky, S. Pospisil, "Radiation hardness properties of full-3D active edge silicon sensors," *Nucl. Instr. Meth. Phys. Res.*, vol. 587, no. 2-3, pp. 243-249, 2008.

[3] M. Lozano, F. Campabadal, C. García, S. Gonzalez-Sevilla, C. Lacasta, V. Lacuesta, S. Martí, M. Miñano, G. Pellegrini, M. Ullán, J.M. Rafí, "Ultimate limits for the radiation hardness of silicon strip detectors for sLHC," *Nucl. Instr. Meth. Phys. Res.*, vol. 581, no. 1-2, pp. 365-367, 2007.

[4] S. Diez, Ullán, F. Campabadal, M. Lozano, G. Pellegrini, D. Knoll, B. Heinemann, "SiGe bipolar transistors for harsh radiation environments," *Proc. Spanish Conference on Electron Devices*, art. no. 4271193, pp. 158-161, 2007.

[5] T.H. Lee, H.D. Kim, S.W. Park, "Front-end electronics for high rate neutron counters: Its performance and radiation hardness improvement," *IEEE Nuclear Science Symposium Conference Record*, 3, pp. 1423-1427, 2004.

[6] M. Deveaux, G. Claus, G. Deptuch, W. Dulinski, Y. Gornushkin, M. Winter, "Neutron radiation hardness of monolithic active pixel sensors for charged particle tracking", *Nucl. Instr. Meth. Phys. Res.,* vol. 512, no. 1-2, pp. 71-76, 2003.

[7] W. Adam, C. Bauer, E. Berdermann, P. Bergonzo, F. Bogani, E. Borchi, A. Brambilla, M. Bruzzi, C. Colledani, J. Conway, W. Dabrowski, P. Delpierre, A. Deneuville, W. Dulinski, B. Van Eijk, A. Fallou, F.

Fizzotti, F. Foulon, M. Friedl, K.K. Gan, E. Gheeraert, E. Grigoriev, G. Hallewell, R. Hall-Wilton, S. Han, F. Hartjes, J. Hrubec, D. Husson, H. Kagan, D. Kania, J. Kaplon, C. Karl, R. Kass, K.T. Knöpfle, M. Krammer, A. Logiudice, R. Lu, P.F. Manfredi, C. Manfredotti, R.D. Marshall, D. Meier, M. Mishina, A. Oh, L.S. Pan, V.G. Palmieri, M. Pernicka, A. Peitz, S. Pirollo, P. Polesello, K. Pretzl, V. Re, J.L. Riester, S. Roe, D. Roff, A. Rudge, S. Schnetzer, S. Sciortino, V. Speziali, H. Stelzer, R. Stone, R.J. Tapper, R. Tesarek, G.B. Thomson, M. Trawick, W. Trischuk, E. Vittone, A.M. Walsh, R. Wedenig, P. Weilhammer, H. Ziock, M. Zoeller, "Review of the development of diamond radiation sensors," *Nucl. Instr. Meth. Phys. Res.*, vol. 434, no. 1, pp. 131-145, 1999.

[8] E. Dupont-Nivet, E. Delagnes, J.L. Leray, J.L. Martin, J. Montaron, J.P. Blanc, E. Delevoye, J. Gauthier, J. de Pontcharra, R. Truche, E. Beuville, M. Dentan, N. Fourches, "Hardened technology on SOI for analog devices," First European Conference on Radiation and Its Effects on Devices and Systems - RADECS 91, pp. 211-214, 1992.

[9] D. Briand, O. Guenat, B. van der Schoot, T. Hirata, N. F. de Rooij, "Micro-hotplate, a useful concept for gas sensing, fluidics and space applications," Proc. 198 Electrochemical Society Meeting 2000-19, pp. 151–157, 2000.

[10] J. Laconte, C. Dupont, D. Flandre, J.-P. Raskin, "SOI CMOS compatible low-power microheater optimization for the fabrication of smart gas sensors," IEEE Sensors J., vol. 3, no. 4, pp. 670-680, 2004.

[11] P. Francis, A. Terao, B. Gentinne, D. Flandre, J.-P. Colinge, "SOI technology for high-temperature applications," Electron Devices Meeting, 1992. IEDM '92. Technical Digest., International, pp. 353-356, 1992.

[12] E._H. Boufouss, L.A. Francis, V. Kilchytska, P. Gérard, P. Simon, D. Flandre "Ultra-low power high temperature and radiation hard complementary metal-oxide-semiconductor (CMOS) silicon-on-insulator (SOI) voltage reference," Sensors, vol. 13, no. 12, pp. 17265–17280, 2013.

[13] M. Graf, D. Barrettino, H. P. Baltes, A. Hierlemann, CMOS hotplate chemical microsensors. Springer-Verlag Berlin Heidelberg, 2007.

[14] P. K. Guha, S. Z. Ali, C.C.C. Lee, F. Udrea, W.I. Milne, T. Iwaki, J.A. Covington, J.W. Gardner, "Novel design and characterisation of SOI CMOS micro-hotplates for high temperature gas sensors," Sens. Act. B, vol. 127, pp. 260–266, 2007.

[15] M. Silindir, A.Y. Özer, "Sterilization methods and the comparison of e-beam sterilization with gamma radiation sterilization," FABAD J. Pharm. Sci., vol. 34, pp. 43–53, 2009.

[16] [Trends in radiation sterilization of health care products], International Atomic Energy Agency, Vienna (2008)

[17] T. R. Oldham, F.B. McLean, "Total ionizing dose effects in MOS oxides and devices," IEEE Trans. Nucl. Sci., vol. 50, no. 3, pp. 483–499, 2003.

[18] H.R. Shea, "Effects of radiation on MEMS," Proc. SPIE 7928, Reliability, Packaging, Testing, and Characterization of MEMS/MOEMS and Nanodevices X, 79280E, 2011.

[19] P. Gkotsis, V. Kilchytska, C. Fragkiadakis, P.B. Kirby, J.-P. Raskin, L.A. Francis, "Effects of fast neutrons on the electromechanical properties of materials used in microsystems," J. Microelectromech. Syst., vol. 21, pp. 1471–1483, 2012.

[20] A. De Luca, V. Pathirana, S.Z. Ali, F. Udrea, "Silicon on insulator thermodiode with extremely wide working temperature range," Proc. 17th International Conference on Solid-State Sensors, Actuators and Microsystems (TRANSDUCERS & EUROSENSORS XXVII), pp. 1911-1914, 2013.

[21] K. Bernier. *An Intense Fast Neutron Beam in Louvain-la-Neuve*. (1997). [Online]. Available: http://www.cyc.ucl.ac.be

[22] *Alanine Dosimeter Reader*. [Online]. Available: http://www.bruker-biospin.com/e-scan_alanine.html